Electronic Supplementary Information

Direct growth of cobalt-rich cobalt phosphide catalyst on cobalt foil: an efficient and self-supported bifunctional electrode for overall water splitting in alkaline media

Cheng-Zong Yuan[a], Sheng-Liang Zhong[b], Yi-Fan Jiang[a], Zheng Kun Yang[a], Zhi-Wei Zhao[a], Sheng-Jie Zhao[a], Nan Jiang[a] and An-Wu Xu[a]*

[a] Division of Nanomaterials and Chemistry, Hefei National Laboratory for Physical Sciences at Microscale, University of Science and Technology of China, Hefei 230026, China.

[b] College of Chemistry and Chemical Engineering, Jiangxi Normal University, Nanchang 330022, P. R. China

*To whom correspondence should be addressed.

Email: anwuxu@ustc.edu.cn.

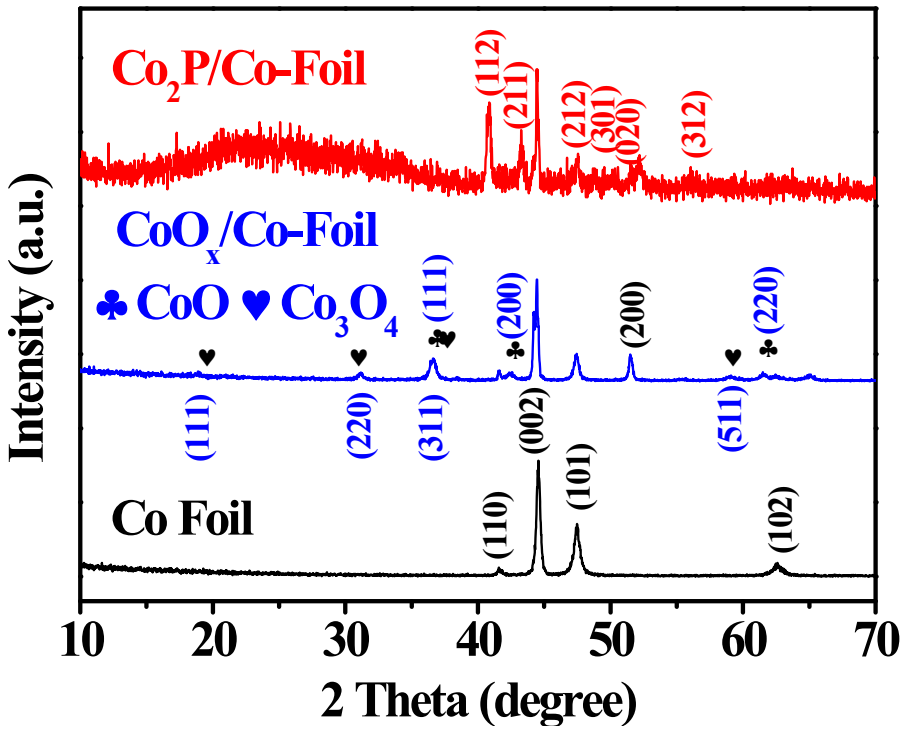

Fig. S1 Powder XRD patterns of Co foil, CoO_x/Co-Foil and Co_2P/Co-Foil electrodes.

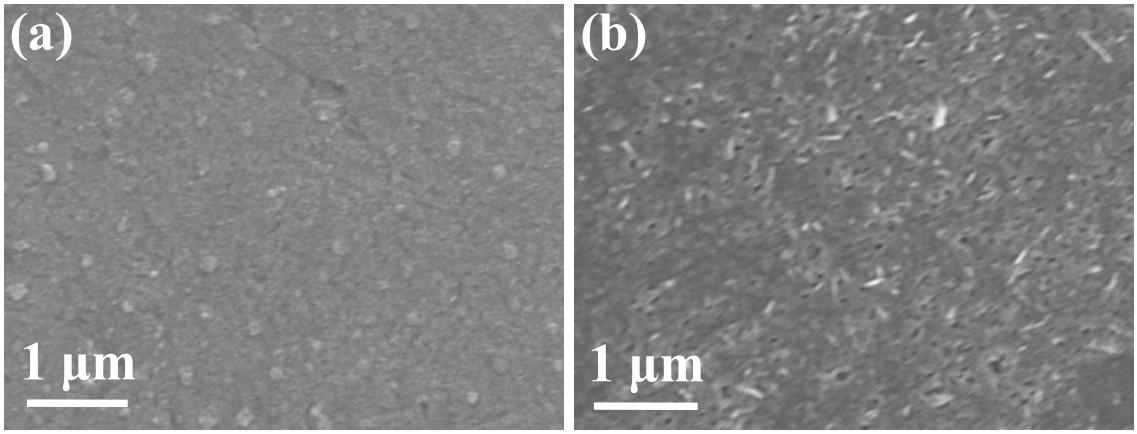

Fig. S2 Scanning electron microscope (SEM) images of (a) Co foil, (b) CoO_x/Co-Foil electrode.

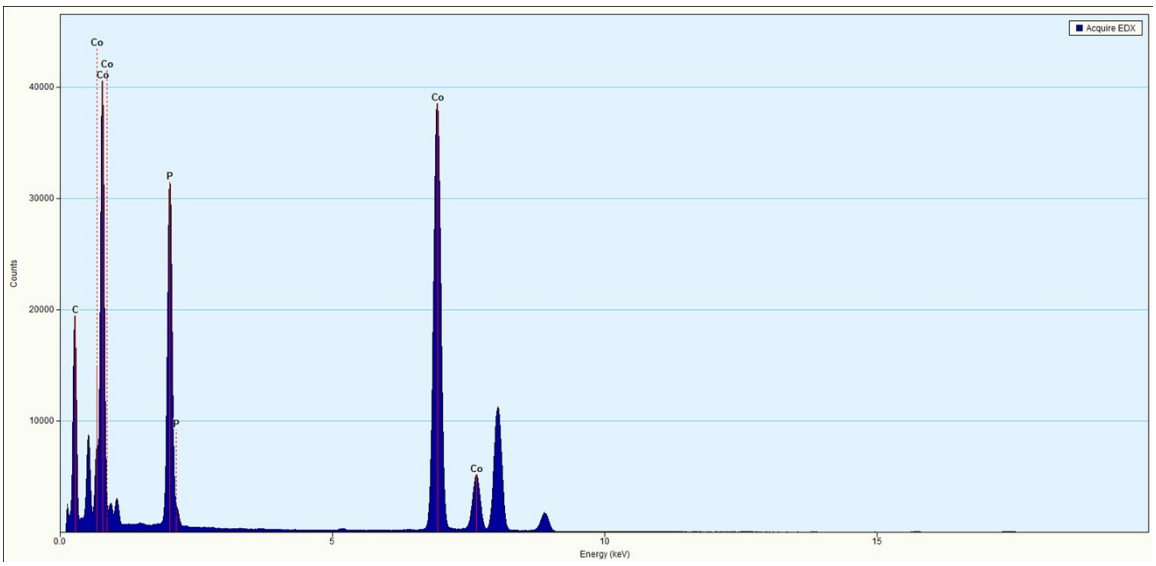

Fig. S3 EDS spectrum of the as-made Co_2P particles peeled off from Co_2P/Co-Foil surface.

Table S1 Ratios of P and Co elements in the obtained Co_2P particles estimated from EDS analysis.

Element	Atomic %	Weight %	Uncert. %
P	31.12	20.03	0.04
Co	64.36	78.83	0.10

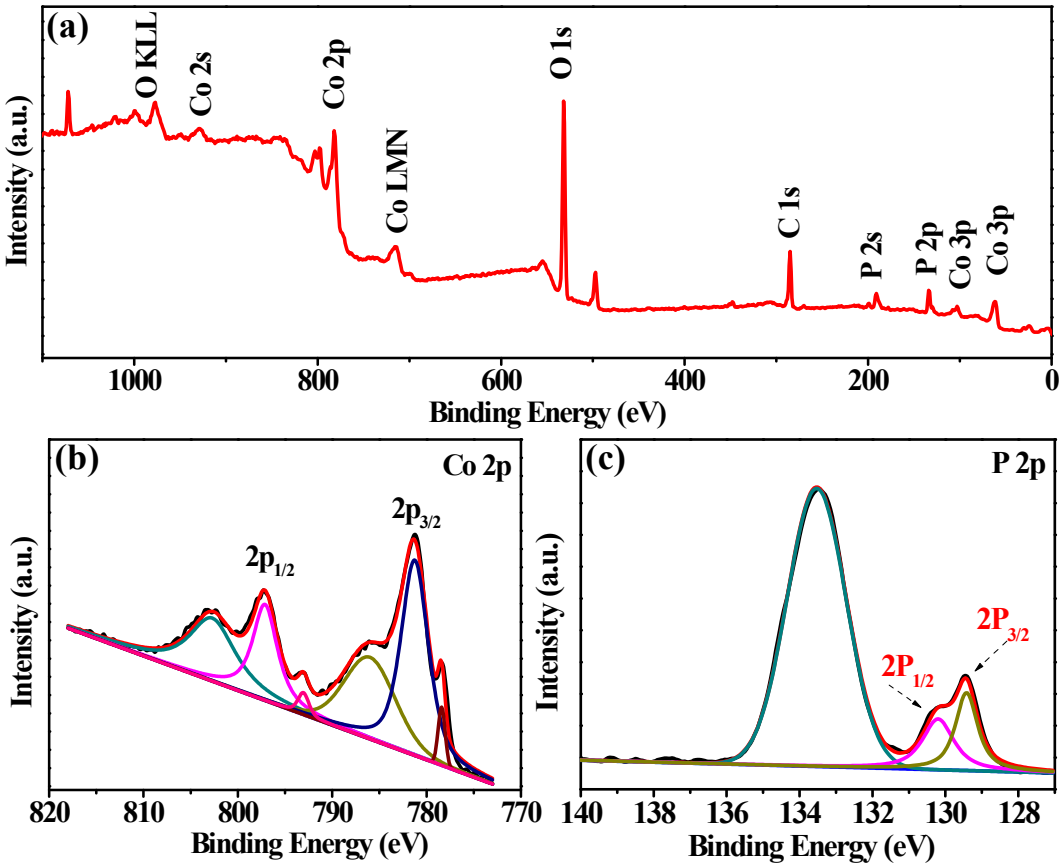

Fig. S4 (a) XPS survey spectra of Co_2P particles peeled off from the surface of Co_2P/Co-Foil. (b) Co 2p and (c) P 2p narrow scans.

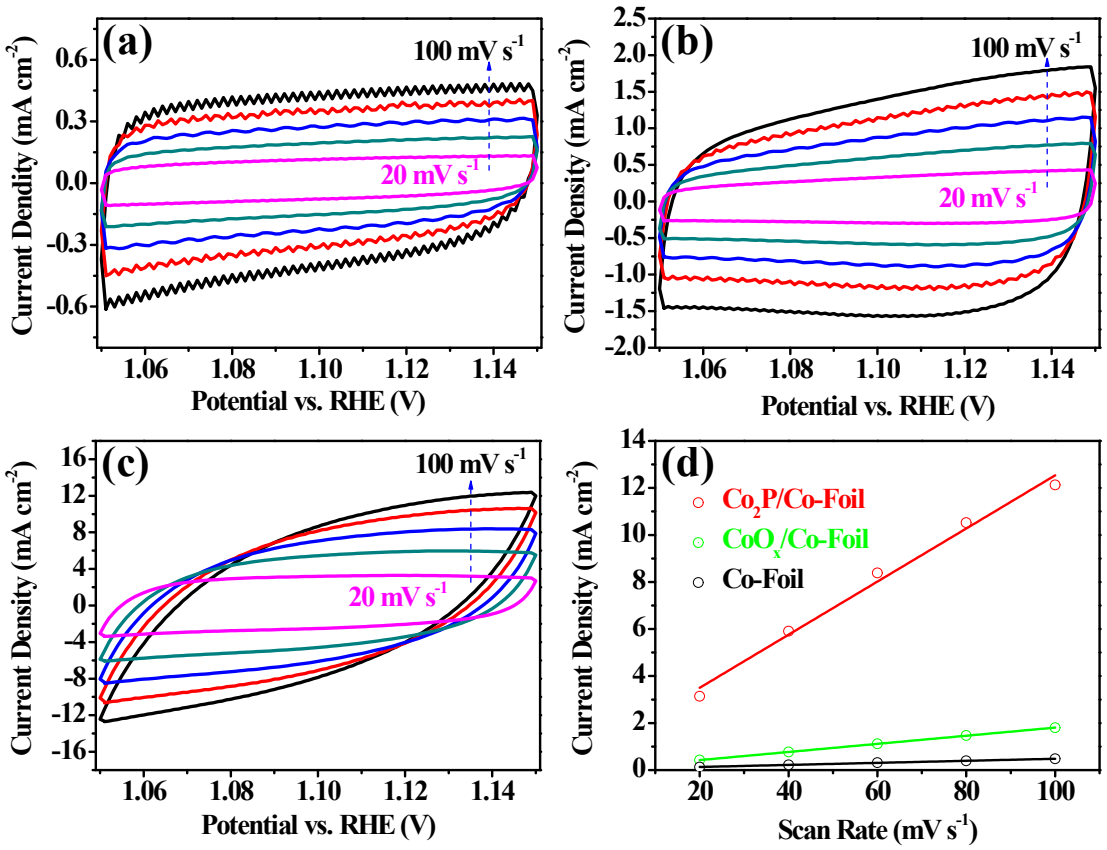

Fig. S5 (a), (b) and (c) Cyclic voltammograms (CVs) of Co foil, CoO_x/Co-Foil and Co_2P/Co-Foil electrodes measured at different scan rates from 20 to 100 mV s^{-1}. (d) Plots of the current density at 1.14 V vs. the scan rate, where the C_{dl} values of Co-Foil, CoO_x/Co-Foil and Co_2P/Co-Foil are 4, 17.3 and 113 mF/cm^2, respectively.

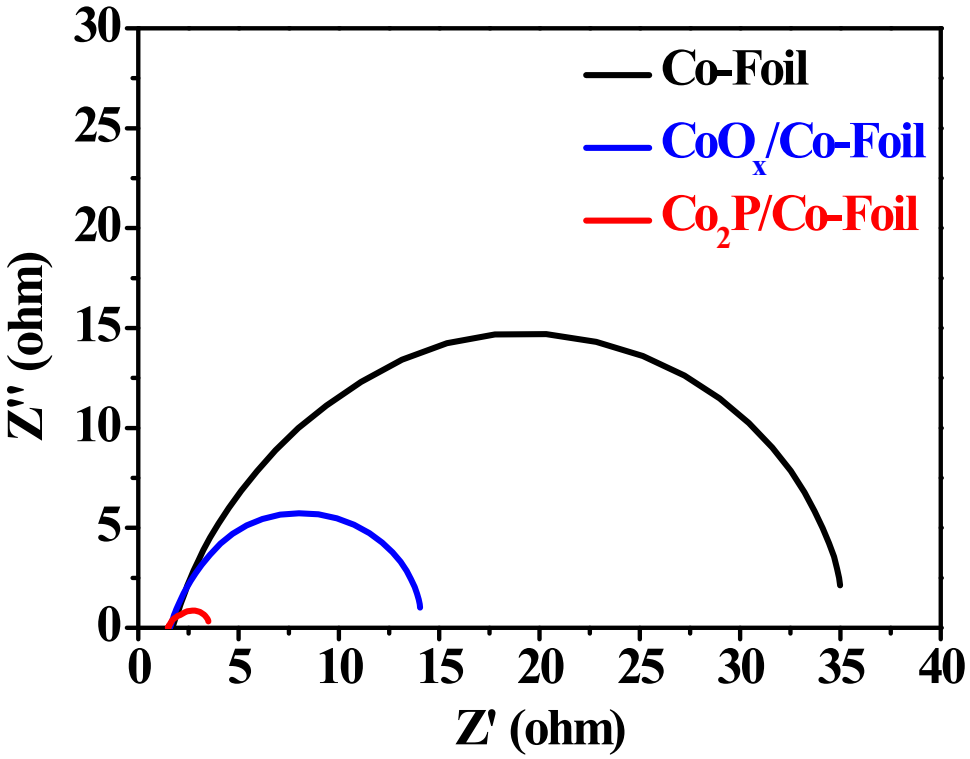

Fig. S6 Electrochemical impedance spectra (EIS) for OER of Co-Foil, CoO_x/Co-Foil and Co_2P/Co-Foil electrodes recorded at 1.56 V vs. RHE.

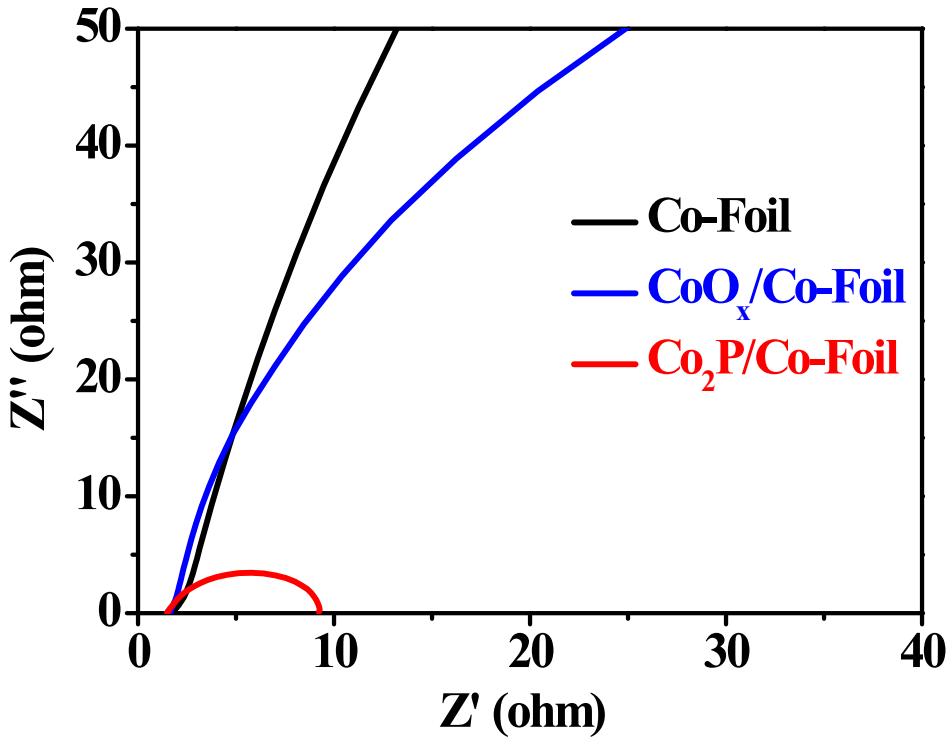

Fig. S7 Electrochemical impedance spectra (EIS) for HER of Co-Foil, CoO_x/Co-Foil and Co_2P/Co-Foil electrodes recorded at -0.16 V vs. RHE.

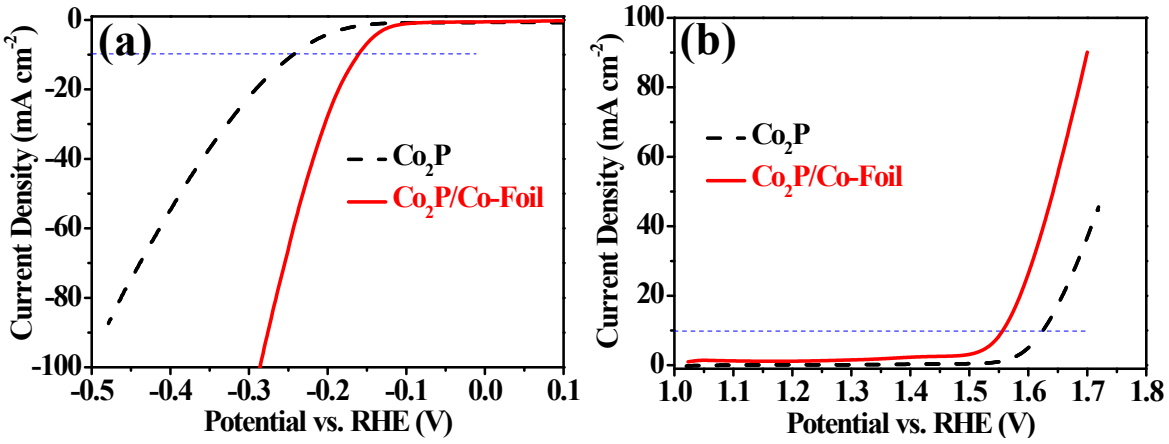

Fig. S8 (a) HER polarization curves and (b) OER polarization curves of Co_2P particles samples peeled off from Co_2P/Co-Foil and the integrated Co_2P/Co-Foil electrode.

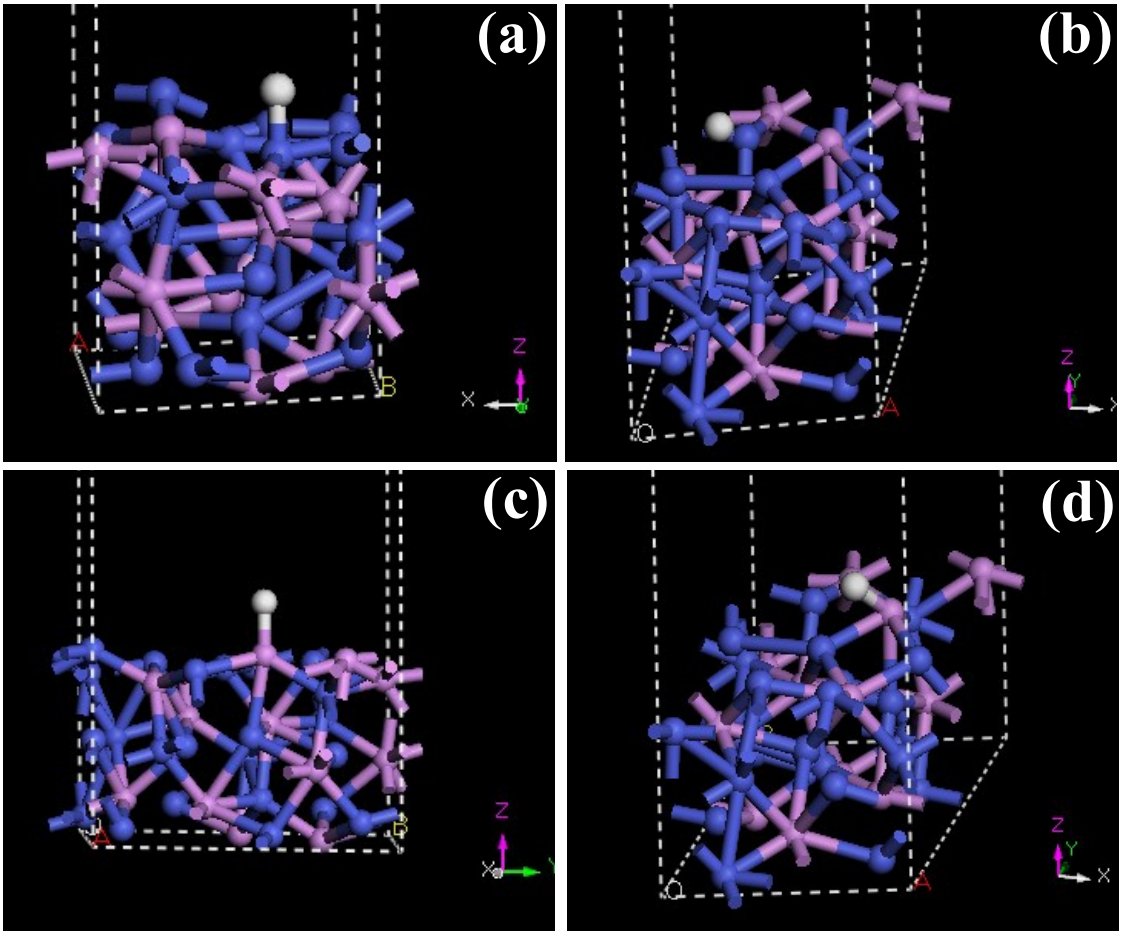

Fig. S9 The corresponding side view of configuration of (a) hydrogen absorbed at the sites on the top of the Co atoms on (112) surface of Co_2P, (b) the bridge sites of Co-Co, (c) the sites on the top of the P atoms, (d) the bridge sites of P-Co.

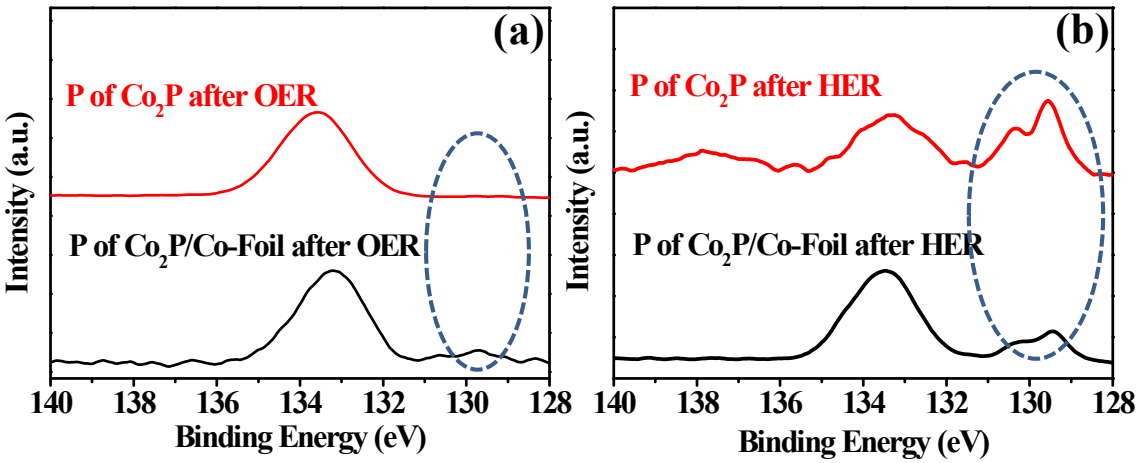

Fig. S10 The XPS P 2p spectra of Co_2P nanoparticles peeled off from the Co_2P/Co-Foil and Co_2P/Co-Foil electrode after OER and HER test.

To further verify the synergistic effect between Co_2P and Co-Foil, XPS spectra of Co_2P nanoparticles peeled off from Co_2P/Co-Foil electrode and Co_2P/Co-Foil after HER and OER were performed and shown in Fig. S10. According to the P 2p spectra of Co_2P and Co_2P/Co-Foil after HER and OER, it is clear that the peak intensity at 130 eV (belongs to phosphate) of Co_2P increased higher than that of Co_2P/Co-Foil and the perks at 129.3 eV (P $2p_{3/2}$) and 130.1 eV (P $2p_{1/2}$) (belong to phosphide) reduced more than that of Co_2P/Co-Foil after OER. Moreover, after HER the peaks of Co_2P at 129.3 eV (P $2p_{3/2}$) and 130.1 eV (P $2p_{1/2}$) increased higher than that of Co_2P/Co-Foil. These results suggest that during the HER and OER process, there are much electron transfer between Co_2P and Co-Foil, confirming the synergistic effect between Co_2P and Co-Foil, which is in line with the observed activity.

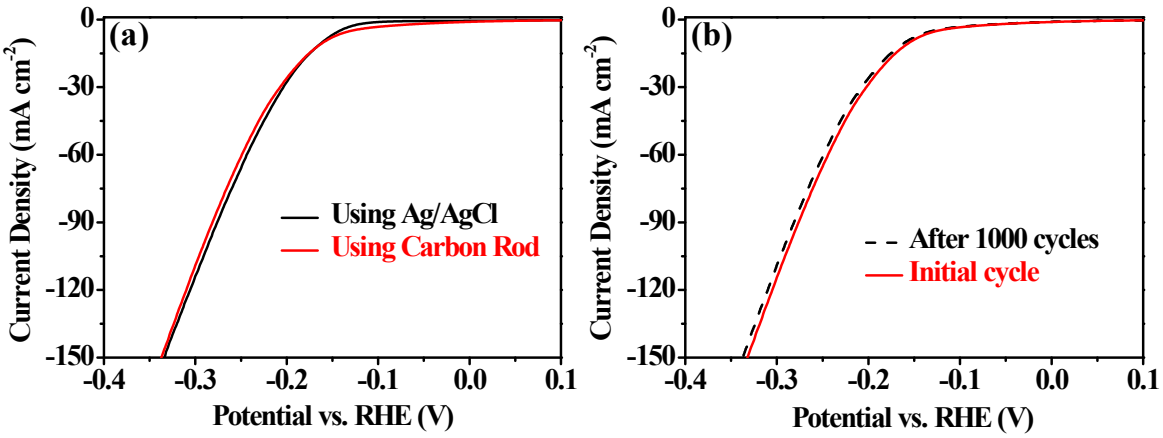

Fig. S11 Electrochemical HER activities of the sample in 1 M KOH solution. (a) Polarization curves tested using the Ag/AgCl electrode and carbon rod as the counter electrode, respectively. (b) The stability of the obtained Co_2P/Co-Foil electrode tested using the carbon rod as the counter electrode.

Recently, Johnny C. Ho et al. (DOI 10.1039/c5ta02551f) verified that the dissolution of Pt was observed when Pt is utilized as the counter electrode. It more likely that the high activity observed is just Pt contamination on the electrode surface, especially in the stability testing process. Therefore, to eliminate influence of Pt, we conducted the experiments (activity and stability) using the carbon rod as the counter electrode and the results were shown in Fig S11, which confirm that the Pt has little influence on the activity of our Co_2P/Co-Foil electrode.

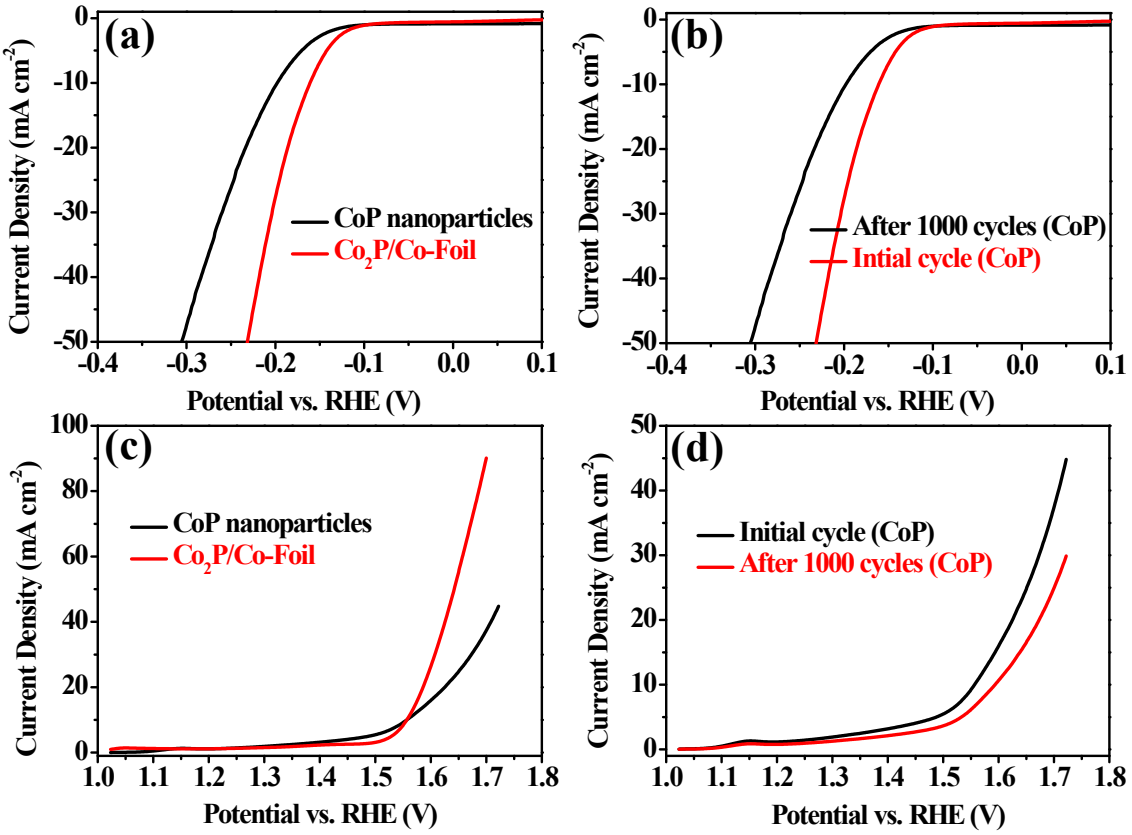

Fig. S12 (a) Electrochemical HER activities polarization curves of CoP nanoparticles and the Co_2P/Co-Foil electrode in 1M KOH. (b) Linear sweep voltammograms towards HER of the CoP nanoparticles obtained before and after 1000 potential cycles with the scan rate of 5 mV s^{-1}. (c) OER polarization curves of CoP nanoparticles and the Co_2P/Co-Foil electrode. (d) Linear sweep voltammograms towards OER of the CoP nanoparticles obtained before and after 1000 potential cycles.

To reveal the Co role in this system, CoP nanoparcitles were prepared using the reported method[1] and corresponding performances were tested and shown in Fig. S12. These results reveal that the rich Co in this catalyst not only improves catalytic activities, but also makes the catalyst more stable during

the OER and HER process. The reasonable explanation is that cobalt-rich cobalt phosphides are nonstoichiometric, leading to more and significant metal-metal bonding in this catalyst, which can effectively enhance the electrical conductivity and make the catalyst more durable.

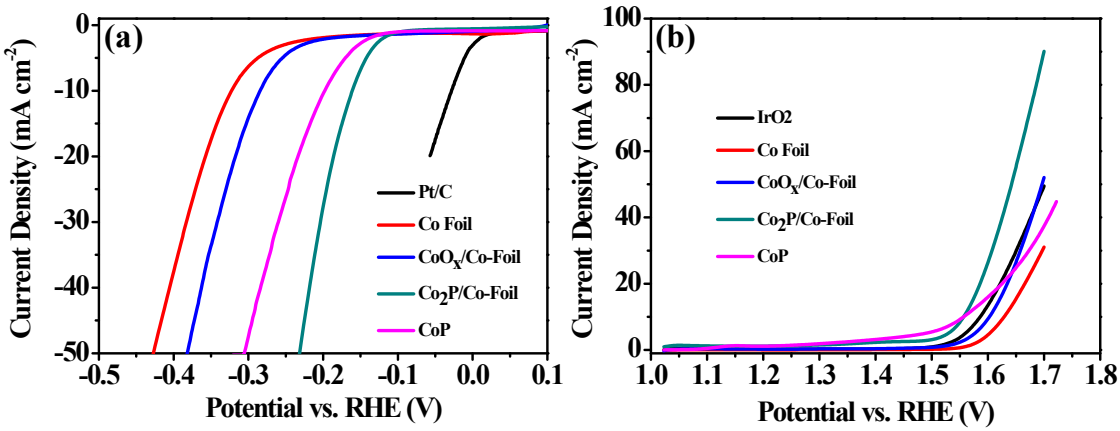

Fig. S13 Electrochemical HER (a) and OER (b) activities polarization curves of the Co_2P/Co-Foil electrode, CoO_x/Co-Foil electrode, Co-Foil electrode, CoP nanoparticles and IrO_2 in 1M KOH. with the scan rate of 5 mV s^{-1}.

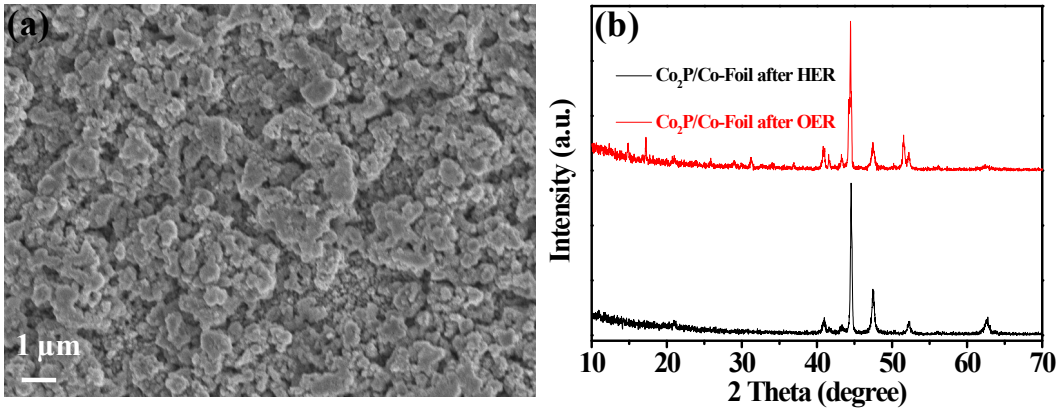

Fig. S14 (a) Scanning electron microscope (SEM) image and (b) XRD pattern of Co_2P/Co-Foil electrode after water splitting test.

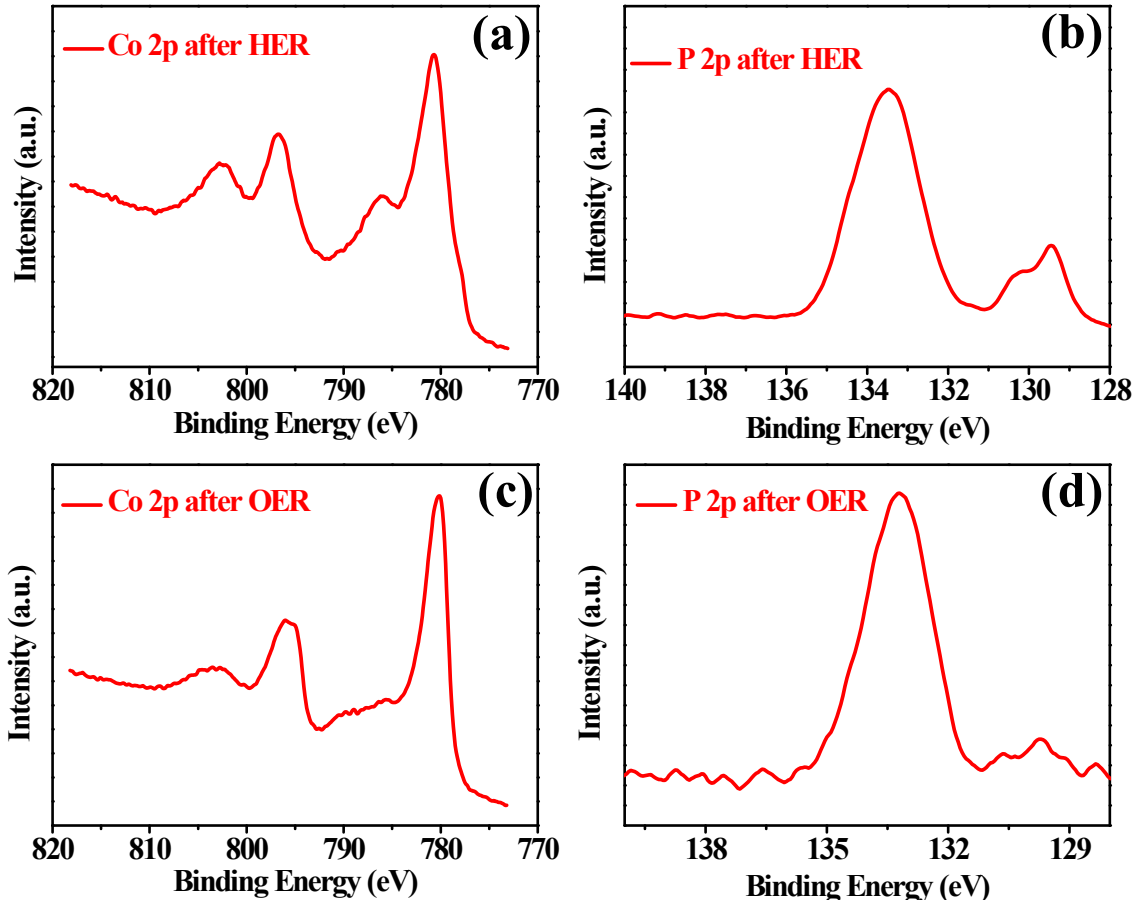

Fig. S15 The XPS spectra of Co_2P/Co-Foil electrode after HER or OER test.

Table S2 The absorption energy of H at the different sites on the (112) surface of Co_2P.

Sites	Energy (eV)
Co	0.480167
Co-Co	-0.481073
P	0.29206
P-Co	-0.486703

Table S3 Comparison of OER performance in alkaline media of some transition metal-based electrocatalysts.

Catalyst	Tafel Slope (mV/dec)	η(@10 mA/cm^2)	Electrolyte	Stable time (h)	Ref.
Co_2P/Co-Foil	79	319	1 M KOH	12	This work.
a-CoSe/Ti	69	292	1 M KOH	25	*Chem. Commun.*, 2015, **51**, 16683.[2]
Mn_3O_4/Ni foam	86	287	1 M KOH	1000 cycles	*J. Mater. Chem. A*, 2015, **3**, 14101.[3]
Ni-P/Ni foam	179.9	/	1 M KOH	50	*J. Mater. Chem. A*, 2016, **4**, 5639.[4]
Ni_2P/Ni foam	112	295	1 M KOH	12	*ACS Catal.*, 2017, **7**, 103.[5]
Ni42-300/Ni42 steel	71.6	320	0.1 M KOH	5.6	*Adv. Funct. Mater.*, 2016, **26**, 6402.[6]

Table S4 Comparison of HER performance in alkaline media of some transition metal-based electrocatalysts.

Catalyst	Tafel Slope (mV/dec)	η(@10 mA/cm^2)	Electrolyte	Stable time (h)	Ref.
Co_2P/Co-Foil	59	154	1 M KOH	12	This work.
CoP/CC	129	209	1 M KOH	22	*J. Am. Chem. Soc.*, 2014, **136**, 7587.[7]
FeP NAs/CC	146	218	1 M KOH	5000 cycles	*ACS Catal.*, 2014, **4**, 4065.[8]
CuCuO-NWs/Ni foam	132	140	1 M KOH	50	*Adv. Funct. Mater.*, 2016, **26**, 8555.[9]
$NiCo_2S_4$/Ni foam	58.9	210	1 M KOH	50	*Adv. Funct. Mater.*, 2016, **26**, 4661.[10]
Ni_3S_2/Ni foam	118	123	1 M KOH	10	*Int. J. Hydrogen Energy*, 2015, **40**, 4727.[11]
Ni_2P/NF	60	93	1 M KOH	24	*Nano Lett.*, 2016, **16**, 7718.[12]

References

1. C. Zhang, Y. Huang, Y. F. Yu, J. F. Zhang, S. F. Zhuo and B. Zhang, *Chem. Sci.*, 2017, **8**, 2769−2775.

2. T. T. Liu, Q. Liu, A. M. Asiri, Y. L. Luo and X. P. Sun, *Chem. Commun.*, 2015, **51**, 16683−16686.

3. M. Q. Yu, Y. H. Li, S. Yang, P. F. Liu, L. F. Pan, L. Zhang and H. G. Yang, *J. Mater. Chem. A*, 2015, **3**, 14101−14104.

4. X. G. Wang, W. Li, D. H. Xiong and L. F. Liu, *J. Mater. Chem. A*, 2016, **4**, 5639−5646.

5. P. W. Menezes, A. Indra, C. Das, C. Walter, C. Göbel, V. Gutkin, D. Schmeiβer and M. Driess, *ACS Catal.*, 2017, **7**, 103−109.

6. H. Schäfer, D. M. Chevrier, P. Zhang, J. Stangl, K. Müller-Buschbaum, J. D. Hardege, K. Kuepper, J. Wollschläger, U. Krupp, S. Dühnen, M. Steinhart, L. Walder, S. Sadaf and M. Schmidt, *Adv. Funct. Mater.*, 2016, **26**, 6402−6417.

7. J. Q. Tian, Q. Liu, A. M. Asiri and X. P. Sun, *J. Am. Chem. Soc.*, 2014, **136**, 7587−7590.

8. Y. H. Liang, Q. Liu, A. M. Asiri, X. P. Sun and Y. L. Luo, *ACS Catal.*, 2014, **4**, 4065−4069.

9. M. Kuang, P. Han, Q. H. Wang, J. Li and G. F. Zheng, *Adv. Funct. Mater.*, 2016, **26**, 8555−8561.

10. A. Sivanantham, P. Ganesan and S. Shanmugam, *Adv. Funct. Mater.*, 2016, **26**, 4661−4672.

11. C. Tang, Z. H. Pu, Q. Liu, A. M. Asiri, Y. L. Luo, X. P. Sun, *Int. J. Hydrogen Energy*, 2015, **40**, 4727−4732.

12. H. F. Liang, A. N. Gandi, D. H. Anjum, X. B. Wang, U. Schwingenschlögl and H. N. Alshareef, *Nano Lett.*, 2016, **16**, 7718−7725.